JOURNAL OF CATALYSIS 60, 241–256 (1979)

Crystallization and Metastable Phase Transformations of Zeolite ZSM-5 in the $(TPA)_2O$–Na_2O–K_2O–Al_2O_3–SiO_2–H_2O System

AYSE ERDEM AND L. B. SAND

Chemical Engineering Department, Worcester Polytechnic Institute, Worcester, Massachusetts 01609

Received January 19, 1979; revised April 23, 1979

Zeolite ZSM-5 was synthesized as the only crystalline phase from Na-TPA, and for the first time from the K-TPA, and Na,K-TPA mixed cation systems. As the organic cation/alkali metal cation ratio was decreased in the reaction mixture, metastable phases were found to coexist with ZSM-5. These were an "analcime-like" phase, and a "mordenite" phase in the Na-TPA system, and a "harmotome-like" phase in the K-TPA system. An isothermal metastable phase transformation diagram was developed for the Na-TPA system. A "gismondine-like" phase was added to the metastable phases coexisting with ZSM-5 and the crystallization sequence, mordenite, ZSM-5, analcime was found to change to gismondine, mordenite, ZSM-5, analcime with the addition of alkali metal salts to the reaction mixture. The "apparent activation energies" obtained for ZSM-5 were 25.57 and 19.41 kcal/gmole for nucleation and crystallization, respectively. The synthesis system could be modified as a result of the cation replacements and the exploratory runs with salt additions, to result in pronounced changes in the morphology, i.e., either to yield larger single crystals or crystal aggregates, desired for the commercial applications.

INTRODUCTION

The purpose of this study was to delineate the synthesis conditions for the crystallization of the important catalyst zeolite ZSM-5 in the Na, K-TPA mixed alkali, organic cation base system. Due to the lack of systematic synthesis data reported in the literature on these systems, the objectives of this study were to delineate the phase relationships, both metastable and equilibrium, and to observe changes in the morphology of crystals and changes in the kinetics of crystallization as functions of the TPA/Na/K ratios in the reaction mixture.

Zeolite ZSM-5 is known for its unusually high silica/alumina ratio, reported to approach 100/1 depending on the synthesis conditions (*1*). The properties which make ZSM-5 suitable and important for industrial applications are its exceptionally high degree of thermal and acid stability and high selectivity in certain catalytic conversions. The crystals have an idealized orthorhombic symmetry, the cell constants being $a = 20.1$ Å, $b = 19.9$ Å, and $c = 13.4$ Å (*2*). The adsorption properties resemble those of the intermediate-port zeolites, having 10-membered ring main channels, as the adsorption of *n*-hexane and some cyclohexane implies a port size on the order of 6 Å.

Synthesis of ZSM-5 was reported by Argauer and Landolt (*1*) from the Na-TPA cation system. The range of compositions of the reaction mixtures and product

0021-9517/79/140241-16$02.00/0

crystals are shown in Fig. 1. The temperature range given in the patent was 125 to 175°C, and the reactant materials were silica, approximately 2.20 *N* tetrapropylammonium hydroxide solution, sodium aluminate, and water. In some of the runs, aluminum turnings were added to maintain the silica/alumina ratio. The crystals obtained were reported to be fine crystalline powder, with crystal sizes on the order of 1 μm.

Recently, Meisel *et al.* (*3*) published a work related to the production of gasoline from methanol in one step. The so-called "Mobil Methanol Process" utilizes an organic cation-shape selective zeolite as the catalyst. It is speculated that the zeolite used was ZSM-5; its approximate model of the pore structure is shown in Fig. 2. The reason for this speculation is the similarity in the properties and also the identical, idealized channel system reported for silicalite (*4*), a pure SiO_2 zeolite, implying that silicalite can be regarded as the silica end-member of a series of aluminosilicate compositions, crystallizing in the $(TPA)_2O$–M_2O–Al_2O_3–SiO_2–H_2O system, in which M is the alkali metal cation. This is strongly supported by the similarity in the X-ray powder diffraction patterns of silicalite and ZSM-5 phases as pointed out by Grose and Flanigen (*5*). One may then say that ZSM-5 has a three-dimensional

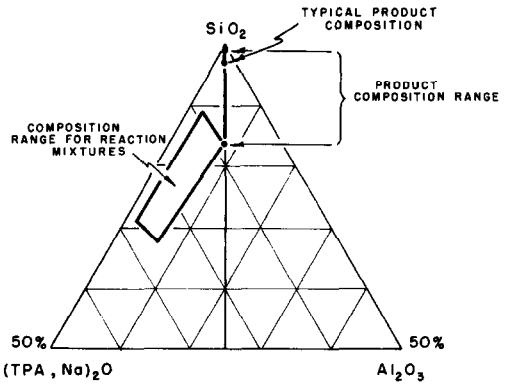

FIG. 1. Ternary diagram for the reaction mixture and product composition ranges (*1*).

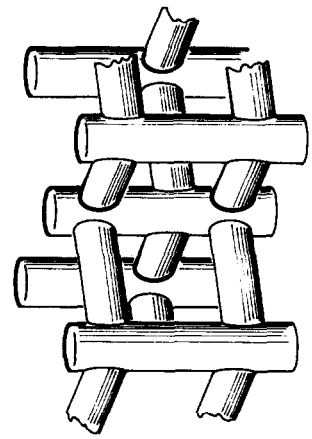

FIG. 2. Possible model of the pore structure of ZSM-5 (*3*).

system of intersecting channels, defined by 10-membered rings, wide enough to adsorb molecules up to 6 Å diameter, and the tetrahedral framework contains a large fraction of five-membered rings of silicon–oxygen tetrahedra. Near-circular, zig–zag channels are present along *a* and *b*, as seen in the figure.

EXPERIMENTAL

Synthesis runs were carried out in modified Morey-type autoclaves of 10 ml capacity at autogeneous pressure. The autoclaves were constructed from aluminum and were lined with Teflon, an inert material which decreases the reaction, adhesion, and nucleation on the surface. For some of the exploratory runs, in which a hard product was obtained, 20-ml reaction vessels were designed and constructed with an additional set of Teflon liners that could be split into two pieces, to overcome the difficulty in taking the product out of the vessel.

The reactant materials used were microfine precipitated silica (QUSO, F20, Philadelphia Quartz Co.), dried aluminum hydroxide gel (F2000, Reheis), reagent grade sodium and postassium hydroxides (Mallinckrodt), 25% tetrapropylammo-

TABLE 1

d-Spacings and Intensities for Na-TPA-ZSM-5

d (Å)	*I*
11.35	29
10.13	22
9.07	8
7.54	10
7.16	7
6.79	8
6.45	11
6.08	13
5.77	10
5.63	11
5.42	5
5.20	6
5.05	8
4.65	9
4.40	12
4.30	13
4.12	7
4.04	11
3.88	100
3.76	52
3.68	31
3.50	10
3.46	13
3.34	13
3.28	8
3.08	12
3.01	16

nium hydroxide solution (Eastman Kodak Co.), and distilled water.

Appropriate amounts of sodium hydroxide, potassium hydroxide, and aluminum hydroxide gel were added to the distilled water to prepare a sodium and/or potassium aluminate solution. In another container the required stoichiometric amount of the quaternary ammonium hydroxide was added to the silica, yielding a viscous TPA-silicate solution. The two solutions were mixed, and the autoclaves were sealed as quickly as possible to prevent TPA absorbing CO_2 gas from the air. The reaction vessels were placed at time zero, on rotating shafts in ovens at temperature and were then rotated at 45 rpm. On termination of the run, the vessels were water-quenched immediately under cold tap water to stop the crystallization process, the solid products were filtered using a Buchner funnel, and dried overnight at 100°C.

The synthesized samples were analyzed by X-ray powder diffraction for qualitative and quantitative phase identification. The unit used was a Philips–Norelco Model 3000 X-ray diffractometer with a scintillation counter and a graphite monochromator attachment, utilizing Ni-filtered CuK_α radiation. For quantitative phase identification, selected reference samples were used, and the percentage crystallization was calculated, with the method of summation of peak intensities. The number of peaks that could be used was limited, to avoid the interference of the different coexisting phases in the same sample, as these phases had overlapping peaks.

The crystalline phases were analyzed for morphology, i.e., crystal size and habit, using a scanning electron microscope (JEOL, Model JSM-43). The samples were mounted on brass pegs, and coated with an Au–Pd evaporated film. Where the resolution of the optical microscope was sufficient, a polarizing microscope (E. Leitz, Trinocular Research Polarizing Microscope, Model Dialux-Pol Df) was used to aid in identification, particularly of minor phases.

RESULTS AND DISCUSSION

Initial exploratory synthesis runs were made in the Na-TPA mixed cation system using the patent information (*1*). Detailed data of the exploratory runs are not included in this paper but are given by Erdem (*6*).

The crystalline phases were identified as ZSM-5, using X-ray powder diffraction analysis. The diffraction pattern of the crystalline phase obtained was found to be very similar to that reported (*2*). The exact peak locations and intensities found by averaging the counts taken for the fixed time of 10 sec, at 0.01° intervals of 2θ Bragg angle are listed in Table 1. The kinetics of crystallization varied consider-

FIG. 3. Scanning electron photomicrograph of Na-ZSM-5 crystals from a reaction mixture with the ratio Na/(Na + TPA) = 0.2.

ably with the silica/alumina ratio and H_2O content of the reaction mixture. The silica/alumina ratio was found to have the strongest effect on the nucleation period, which is a measure of the rate of nucleation; the higher the silica/alumina ratio, the longer the induction period and the slower the nucleation rate. The water content of the reaction mixture was observed to affect the rate of crystallization strongly; the lower the amount of H_2O in the reaction mixture, the higher the crystallization rate, which is the usual expected result.

It was also observed that no crystalline phase formed without the addition of alkali-metal cations; i.e., when TPA was the only cation in the reaction mixture, the product was amorphous.

As a result of the preliminary runs, a reaction mixture composition of 10-(Na, TPA)$_2$O–Al_2O_3–28SiO_2–750H_2O was selected for further studies. Water content was kept at a relatively high level in the reaction mixtures for ease of handling of

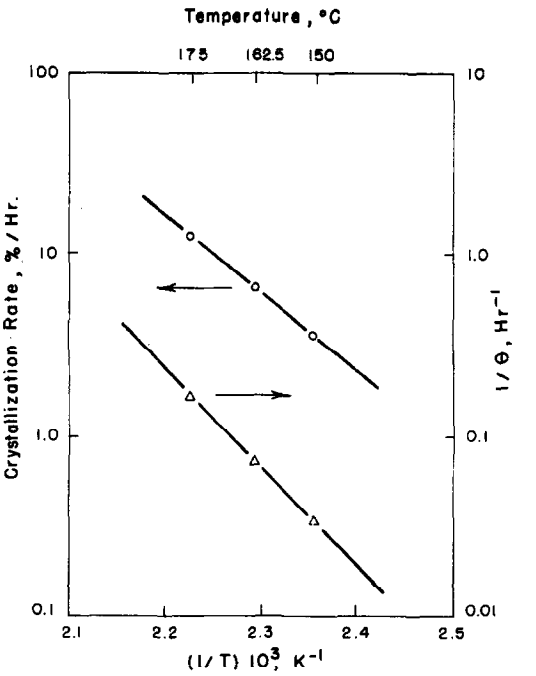

FIG. 4. Dependence of the rate of crystallization and induction period on temperature for zeolite ZSM-5.

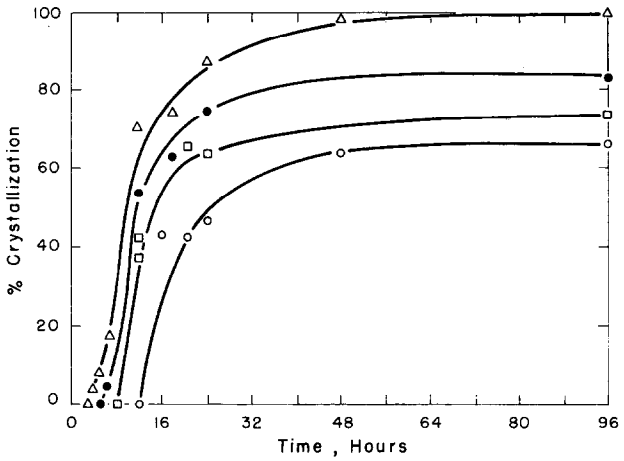

FIG. 5. Effect of the potassium replacement of sodium in the batch mixture on the kinetics of crystallization.

the products, although this increased the time required for crystallization.

The morphology of the crystals of Na-ZSM-5 obtained in this manner are seen in Figure 3. The scanning electron photomicrograph illustrates fine crystalline material of sizes less than 0.5 μm, which is similar to the morphology reported (*1*).

A kinetic study was made for the selected batch composition, to determine the kinetic parameters E_n and E_c, apparent activation energies for nucleation and crystallization, respectively. Nucleation and crystal growth were assumed to be the rate-limiting steps during the induction period and crystallization period, respectively, and the dependence of the rates on temperature, for three synthesis temperatures of 175, 162.5, and 150°C, were expressed by the Arrhenius equation (*6*). Figure 4 illustrates the dependence of the rate of crystallization and induction period on temperature. The calculated values are listed in Table 2, together with those of mordenite, obtained after a similar analysis by Culfaz (*7*), for comparison. This phase

TABLE 2

Apparent Activation Energies for Nucleation and Crystallization, E_n and E_c, of Mordenite (*7*) and ZSM-5

Zeolite	E_n (kcal/ gmole)	E_c (kcal/ gmole)
Mordenite	24	15
ZSM-5 (rotated)	25.57	19.41

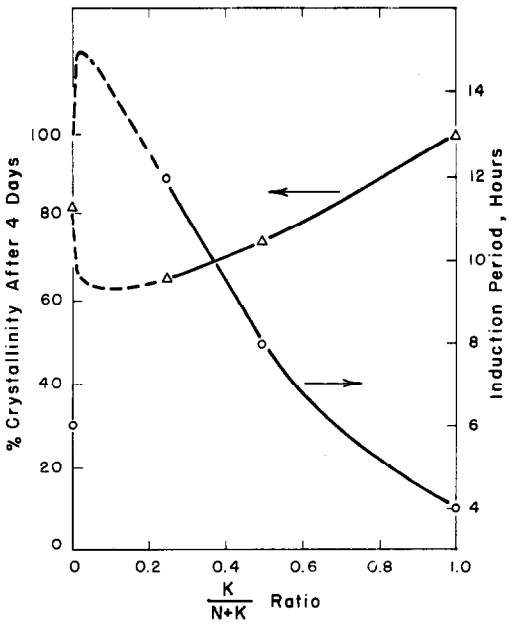

FIG. 6. Variation of the induction period and wt% crystallinity after 4 days with the K/(Na + K) ratio in the batch mixture.

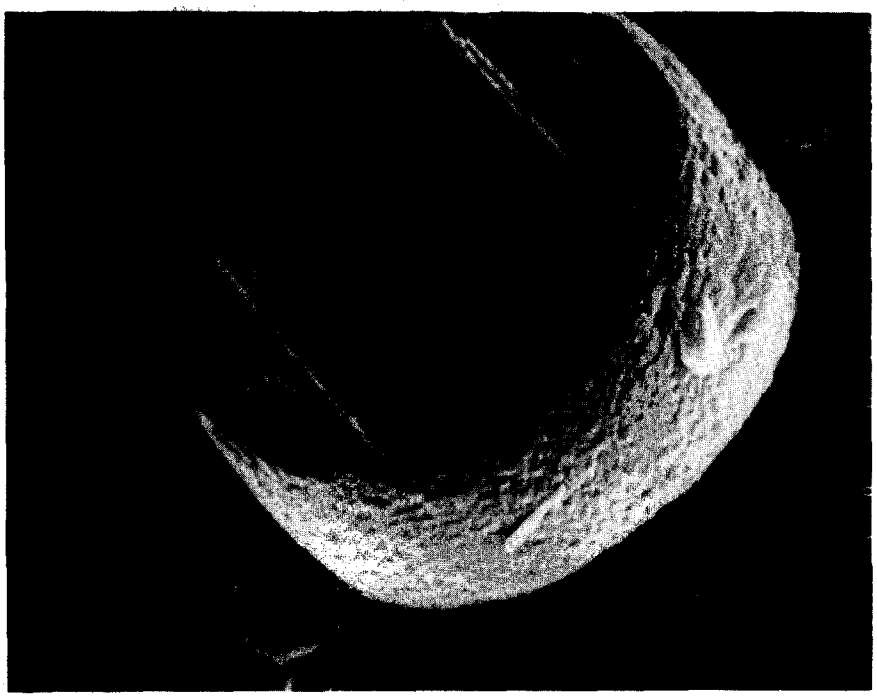

FIG. 7. Scanning electron photomicrograph of Na, K-ZSM-5 crystals from a reaction mixture with the ratios (Na + K)/(Na + K + TPA) = 0.2 and K/(K + Na) = 0.75.

was found to be coexisting with zeolite ZSM-5 under certain conditions of synthesis, which will be discussed later in this paper.

Synthesis of ZSM-5 from a K-TPA mixed cation system had not been reported previously but was accomplished in this study. Potassium replacement of sodium

TABLE 3

d-Spacings and Intensities for K-TPA-ZSM-5

d (Å)	*I*	Å (*d*)	*I*
11.40	29	4.12	7
10.21	23	4.05	10
9.09	6	3.88	100
7.57	11	3.78	48
7.18	7	3.75	48
6.79	8	3.68	32
6.45	12	3.55	5
6.08	12	3.50	10
5.78	10	3.47	17
5.64	11	3.34	20
5.42	5	3.29	11
5.20	6	3.24	10
5.05	8	3.16	6
4.65	8	3.07	14
4.41	12	3.00	21
4.30	14		

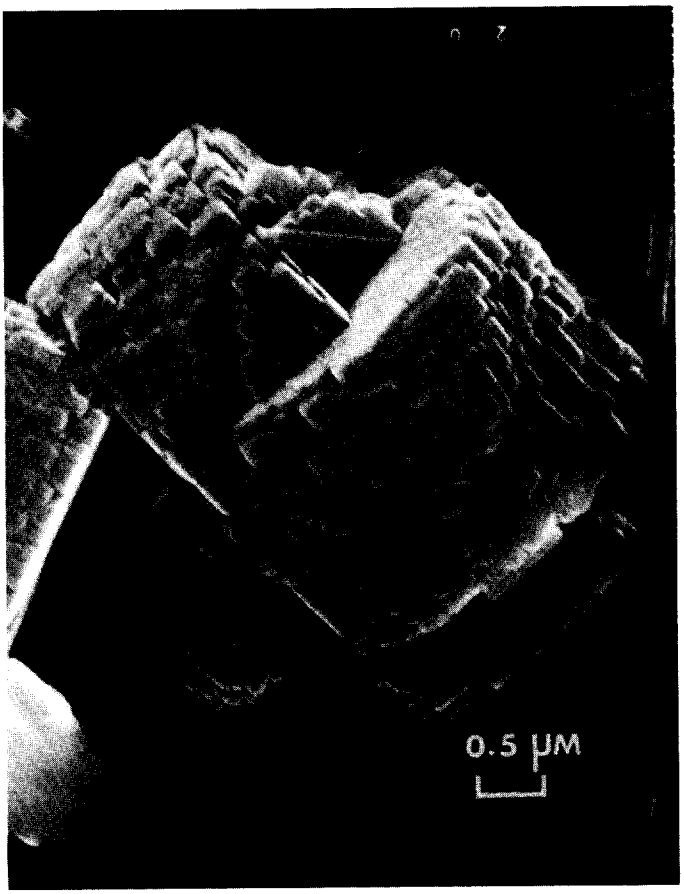

FIG. 8. Scanning electron photomicrograph of K-ZSM-5 crystals from a reaction mixture with the ratio K/(K + TPA) = 0.2.

ions in the reaction mixture, for the same cation/alumina ratio and alkali metal cation/TPA ratio, was found to affect both the kinetics of crystallization and the morphology of the product crystals, without changing the structure, for a certain range of TPA/(TPA + Na + K)

TABLE 4

d-Spacings and Intensities for the "Harmotome-like" Phase

d (Å)	*I*
6.32	100
4.26	4
4.09	6
3.43	7
3.33	7
3.29	5
3.23	6
3.14	30
3.00[a]	5
2.93	20

[a] May be due to the coexisting ZSM-5 phase.

TABLE 5

d-Spacings and Intensities for the "Analcime-like" Phase

d (Å)	*I*
5.60	vs
4.84	s
3.65	m
3.43	vs
2.92	vs
2.79	mw
2.68	ms
2.51	ms
2.42	m

FIG. 9. Scanning electron photomicrograph of the coexisting "harmotome-like" and ZSM-5 phases.

ratios. Effect of the potassium replacement of sodium on the kinetics of crystallization for a batch mixture of $8(TPA)_2O$–$2(Na, K)_2O$–Al_2O_3–$28SiO_2$–$750H_2O$ is seen in Fig. 5 for four different K/(Na + K) ratios. An interesting result is that there seems to be a continuous gradual change in the kinetics for the systems containing both alkali metal cations, Na and K, with the increase in the K/(Na + K) ratio, until the pure potassium end of the reaction mixture series is reached; but

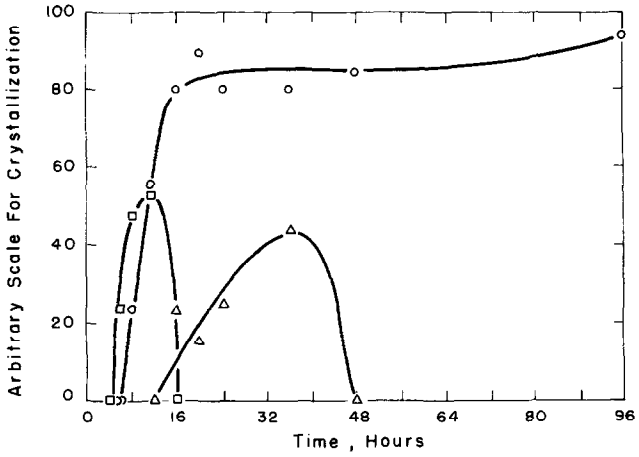

FIG. 10. Crystallization curves showing the metastability of the mordenite and "analcime-like" phases, coexisting with ZSM-5, from a batch composition of $6(TPA)_2O$–$4Na_2O$–Al_2O_3–$28SiO_2$–$750H_2O$.

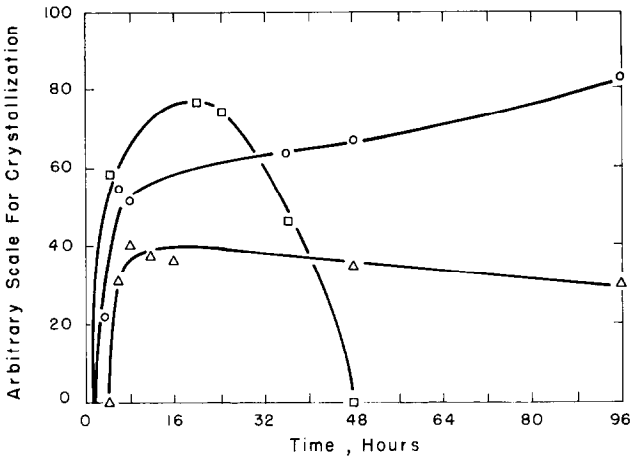

FIG. 11. Crystallization curves for the coexisting phases that form from a batch composition of $4(TPA)_2O$–$6Na_2O$–Al_2O_3–$28SiO_2$–$750H_2O$.

the sodium end of the series has a discontinuity in this dependence.

The higher the K/(Na + K) ratio, the higher the rate of nucleation and the rate of crystallization, as is indicated by the shorter induction period and by the higher slope of the crystallization curves at a fixed conversion, respectively. The induction period and wt% crystallinity after 4 days are plotted against the K/(Na + K) ratio in the batch mixture in Fig. 6. As can be seen from the figure, the increase in both rates is not valid for the initial addition of the potassium ions to the

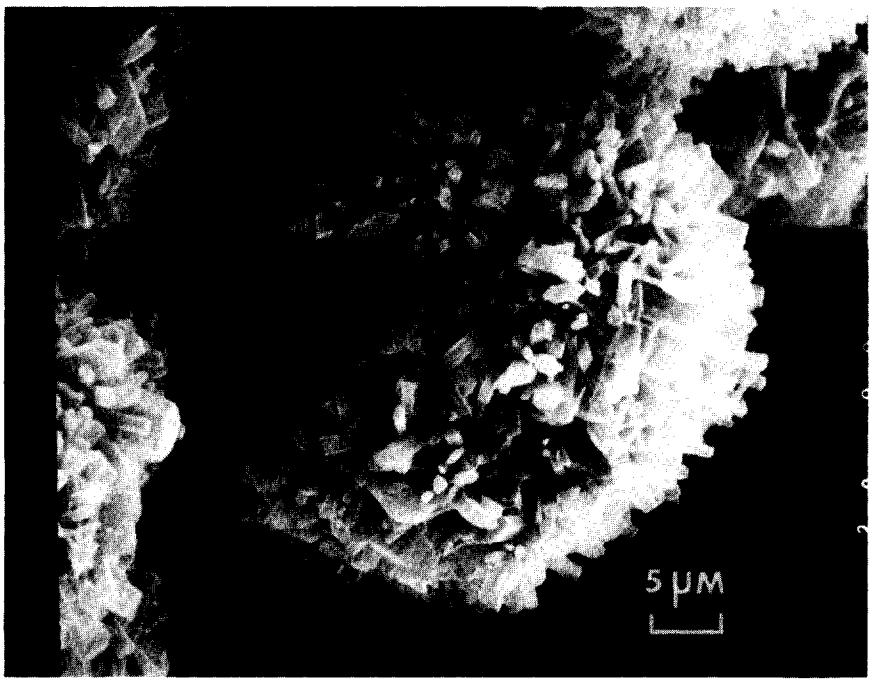

FIG. 12. Scanning electron photomicrograph of the crystal aggregates of mordenite phase.

sodium system. When a very small quantity of potassium is introduced into the Na-TPA batch, both rates experience a decrease. However, further addition of potassium ions increases both rates, so that the values for both rates, and the wt% crystallinity at any fixed time, are much higher for the pure K-TPA reaction mixtures. The reason for this observation could be a potassium selectivity for the building units of the framework structure. A potassium selectivity in both the nuclei formation and crystal growth could explain (i) the increasing rates with increasing K/Na ratios in the Na, K-TPA mixted alkali batches until the pure K end is reached, i.e., for the $0 < K/(Na + K) \leqslant 1$ range, and also (ii) the disturbance at the sodium end; or, in other words, the lower rates of the Na, K-TPA mixed alkali batches than those of the pure sodium batch until a sufficient amount of Na is replaced with potassium. This value seems to be about 70% replacement of the sodium ions for the given synthesis conditions, i.e., the rates of nucleation and crystallization from a reaction mixture with the ratio $K/(Na + K) = 0.7$, are identical to those from the Na-TPA batch, as can be seen in Fig. 6.

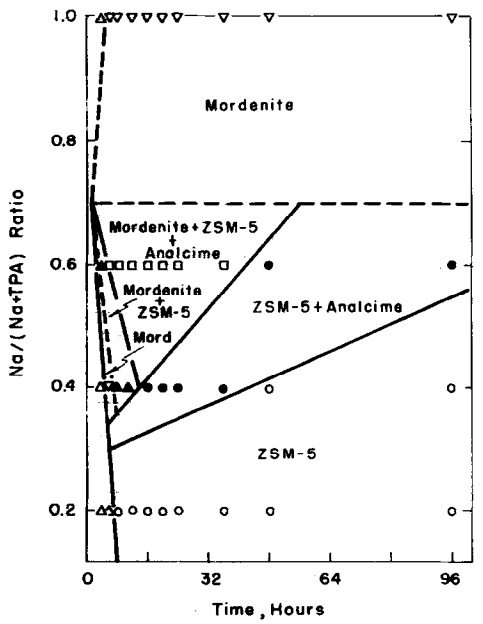

FIG. 13. Isothermal metastable phase transformation diagram for the reaction system $10(TPA,Na)_2O$–Al_2O_3–$28SiO_2$–$750H_2O$ at 175°C.

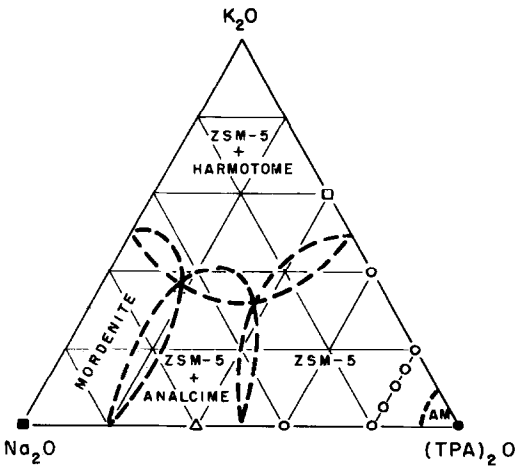

FIG. 14. Ternary composition diagram for the Na_2O–K_2O–$(TPA)_2O$ cation system, showing the stability areas of the phases forming after 4 days, from a reaction mixture of $10(Na,K,TPA)_2O$–Al_2O_3–$28SiO_2$–$750H_2O$.

The very large change in the morphology of the ZSM-5 crystals can be seen from the scanning electron photomicrographs of Figs. 7 and 8 when compared to the Na-TPA–ZSM-5 seen in Fig. 3. Figure 7 shows a ZSM-5 crystal aggregate synthesized from a reaction mixture containing both Na and K cations with a ratio $K/(Na + K) = 0.75$. For the batches in which the K replacement of Na was less than 70%,

TABLE 6

Description of the Reference Samples Used for Quantitative Analysis by X-Ray Powder Diffraction

Phase	Description
Analcime	From Pinnacle Rock, Minas Basin, Nova Scotia
Mordenite	Na-Zeolon, Norton Company
ZSM-5	The ZSM-5 sample, which was highest in crystallinity (*6*)
Phillipsite	Pine Valley, Nevada

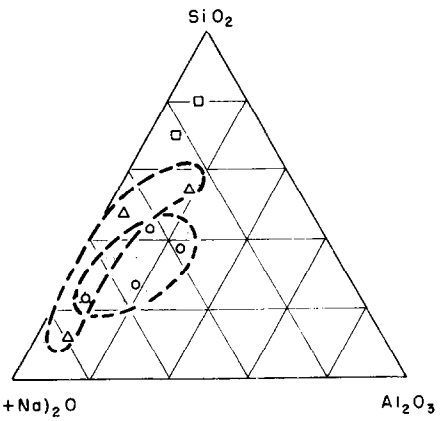

FIG. 15. Ternary diagram showing the reaction mixture compositions for the exploratory runs in the Na–TPA system, and the phases formed after 24 hr.

the change in morphology was not as pronounced; the crystal (or aggregate) sizes were nonuniform and the crystal shape less defined, which is in agreement with the above discussion. Figure 8 shows the ZSM-5 crystals grown from the K-TPA batch. The crystal (aggregate) morphology resembles those of intergrown disks, with sizes in the range of 5 to 10 μm. The increase in the crystal size is quite high, about 10 to 20 times of those of the Na-TPA–ZSM-5 crystals seen in Fig. 3, which might be an important and desired property change for some sorptive and catalytic applications. The exact peak locations and intensities of the X-ray diffraction pattern of K-TPA–ZSM-5 are listed in Table 3.

TABLE 7

d-Spacings and Intensities for the "Gismondine-like" Phase in the Na System

d (Å)	*I*
7.13	43
6.37	12
5.03	35
4.11	52
3.65	11
3.18	100
2.90	16
2.69	55
2.51	12
2.37	16

In both of the Na-TPA and K-TPA cation systems, it was observed that there was a certain range of the organic cation concentrations in the reaction mixtures which yielded ZSM-5 as the only crystalline phase.

In the K-TPA cation system, the organic cation/total cation ratio, i.e., TPA/(K + TPA), was decreased from 0.8 to 0.6 and 0.4. At a ratio of 0.6, ZSM-5 crystallized as a pure phase; whereas, at a ratio of 0.4 a "harmotome-like" phase was found to coexist with ZSM-5. The crystallization curves and the scanning electron photomicrographs are given by Erdem (*6*). Although the crystals resemble the K-TPA–ZSM-5 morphology seen in Fig. 8, they are much less defined in shape and smaller in size.

The X-ray powder diffraction pattern of the "harmotome-like" phase, coexisting with ZSM-5 as the organic cation concentration is decreased in the K-TPA system, is listed in Table 4. The scanning electron micrograph of Fig. 9 illustrates the morphology of the "harmotome-like" phase coexisting with the ZSM-5 crystals. The crystal sizes are on the order of 100 × 15 × 3 μm.

In the Na-TPA system, decreased concentration of the organic cation in the reaction mixture resulted in the coexistence of two metastable phases, identified to be an "analcime-like" phase and a mordenite phase. The mordenite phase had the same X-ray powder diffraction pattern as that reported by Sand *et al.* (*8*) for the synthetic large-port Na-mordenite. The X-ray diffraction pattern of the "analcime-like" phase is listed in Table 5.

Figures 10 and 11 show the metastability of these phases, that form from reaction mixtures with the ratio TPA/(Na + TPA) = 0.6 and 0.4, respectively. The period of time during which these phases coexisted with ZSM-5 increased with decreasing

TPA content of the batch mixture, implying that the phases became relatively more stable.

The coexistence of three different phases in the same sample complicated the quantitative analysis by X-ray powder diffraction. The method of the sum of the peak intensities was limited to the utilization of only two or three peaks for each phase, because of the overlapping peaks found in more than one phase, which could not be used for quantitative analysis to represent a phase. The data on the crystalline phases were not normalized to add up to 100% of the solid phase, because of the observation of an increase in the peak intensities of the ZSM-5 phase even after the disappearance of both of the metastable phases, mordenite and analcime, from the system, implying that there was still some amorphous solid gel left in the solids. As the percentage of the amorphous matter could not be determined with the methods employed and the available data, it was decided to plot the data on an arbitrary scale for crystallization, which is different than the conventional use of percentage crystallization scale. The growth of each phase in the sample was referenced to an external standard. These reference samples are listed in Table 6.

Upon further decrease of the TPA/(Na + TPA) ratio to 0, mordenite was found to be the only crystalline phase forming. The morphology is as seen in Fig. 12. Mordenite crystallizes in the form of near-spherical aggregates in the fluidized size range of 40 to 60 μm.

The data on the effect of the organic cation/alkali-metal cation ratio are used to obtain an isothermal metastable phase transformation diagram, shown in Fig. 13. Amorphous gel converts directly to the ZSM-5 phase for the starting compositions of the ratio Na/(Na + TPA) < 0.3. For the range of 0.3 < Na/(Na + TPA) < 0.34, the "analcime-like" phase forms and dissolves early in the reaction period. For higher values of the above ratio, mordenite forms metastably before the appearance of analcime, and dissolves before the analcime phase disappears. The ZSM-5 nucleation period is between that of mordenite and analcime, and ZSM-5 crystals were observed to coexist with either one or both of these phases, depending on the cation formulation and time of reaction. The close values of the apparent activation

TABLE 8

d-Spacings and Intensities for the "Phillipsite-like" Phase in the K System

d (Å)	*I*
8.30	29
7.19	52
5.42	25
5.03	46
4.31	25
4.10	24
3.67	17
3.53	13
3.44	15
3.25	79
3.19	100
2.96	47
2.75	33
2.69	30
2.56	20
2.37	16

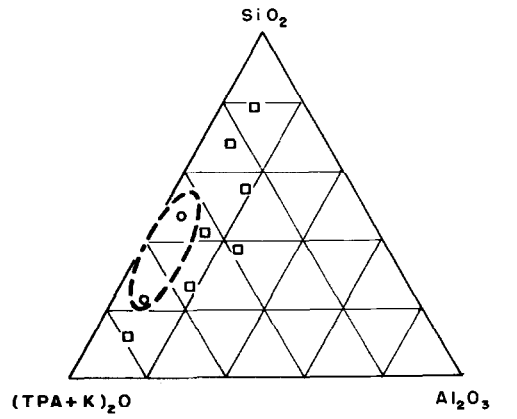

FIG. 16. Ternary diagram showing the reaction mixture compositions for the exploratory runs in the K-TPA system, and the phase formed after 24 hr.

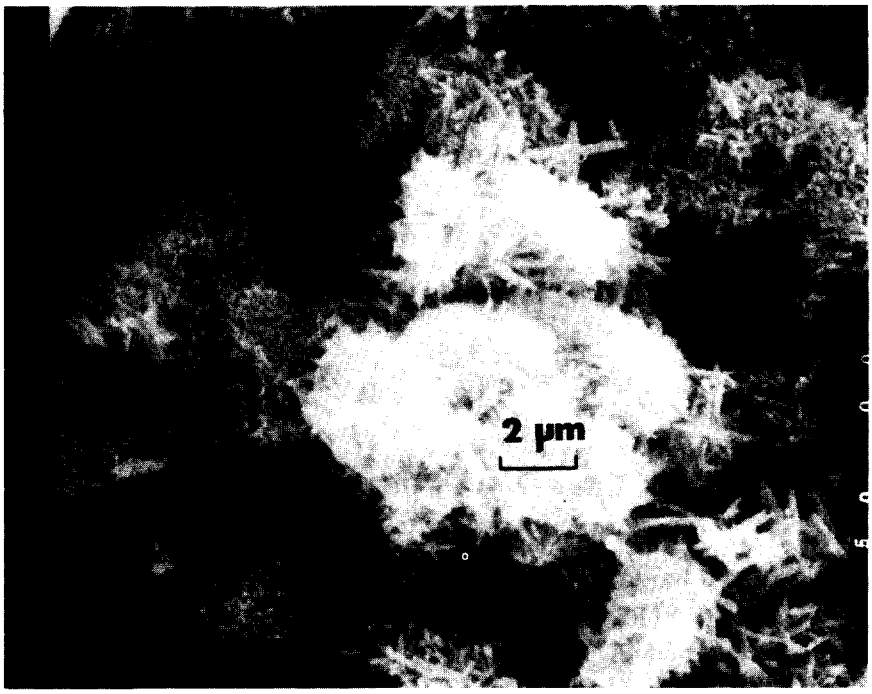

FIG. 17. Scanning electron photomicrograph of the "phillipsite-like" phase.

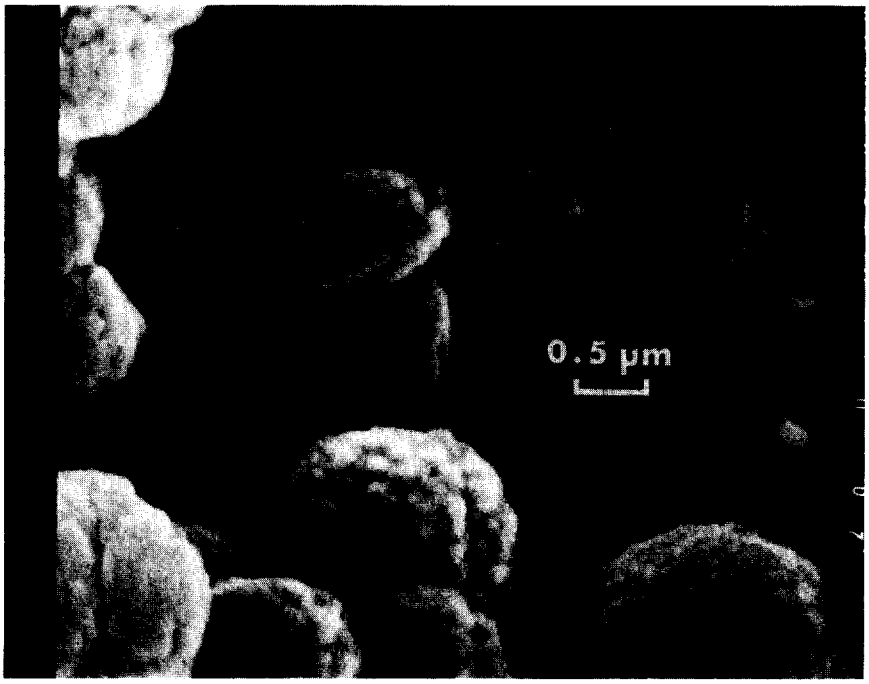

FIG. 18. Scanning electron photomicrograph of the Na-ZSM-5 crystals from a reaction mixture with the ratios Na/(Na + TPA + TBA) = 0.2 and TBA/(TBA + TPA) = 0.25.

energies for nucleation for the mordenite and ZSM-5 phases, the activation energy of mordenite being slightly lower, as seen in Table 2, is in good agreement with the very short reaction time required after the nucleation of mordenite, for the ZSM-5 nuclei formation.

The data on the K-TPA and Na-TPA cation systems, which are discussed above, are combined to give a ternary composition diagram showing the stability areas of the phases forming after 4 days, as is shown in Fig. 14. The stability area of the ZSM-5 phase lies close to the TPA end of the ternary diagram. As the reaction time was limited to 4 days in all of these runs, the phases shown are still accompanied by amorphous matter in certain regions of the ternary composition diagram, where nucleation and crystallization rates are slow. The area of batch formulations yielding ZSM-5 and "analcime-like" phases is expected to decrease with extended reaction times, as implied by the tendency of the "analcime-like" phase to dissolve, which can be seen in Fig. 13. The data for the potassium end of the ternary diagram were not sufficient, and the diagram is left for completion by further studies; it is only an initial attempt to aid in future work.

TABLE 9

d-Spacings and Intensities for the "Hydroxy Sodalite-like" Phase

d (Å)	*I*
9.47[a]	7
6.89[a]	7
6.32	36
5.24	5
4.47	42
3.65	100
3.42	17
3.16	16
2.82	14
2.58	18

[a] Very wide peaks may be due to the presence of some amorphous matter.

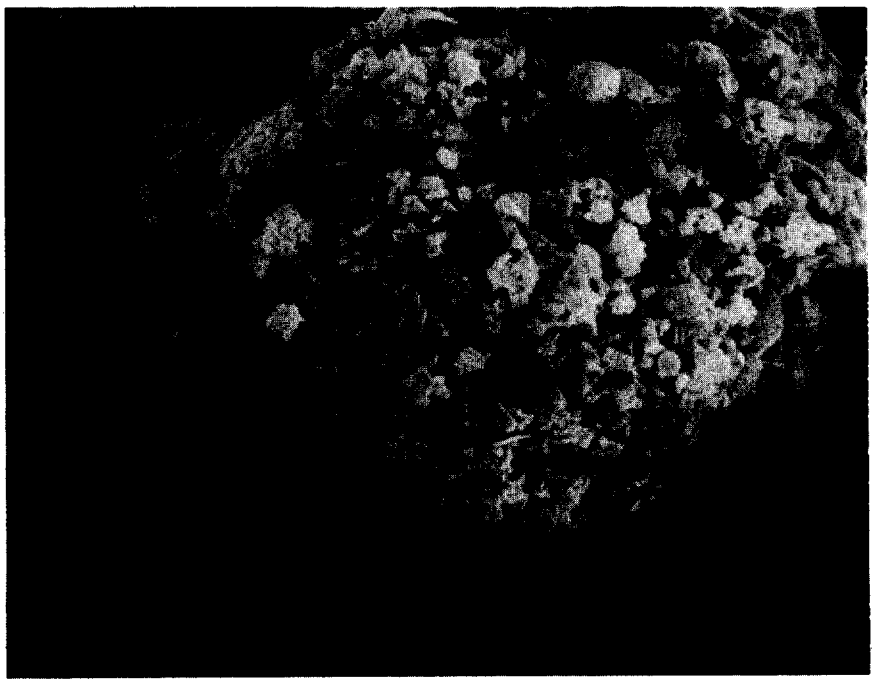

FIG. 19. Scanning electron photomicrograph of the crystal aggregate grown with the addition of NaCl to the reaction mixture.

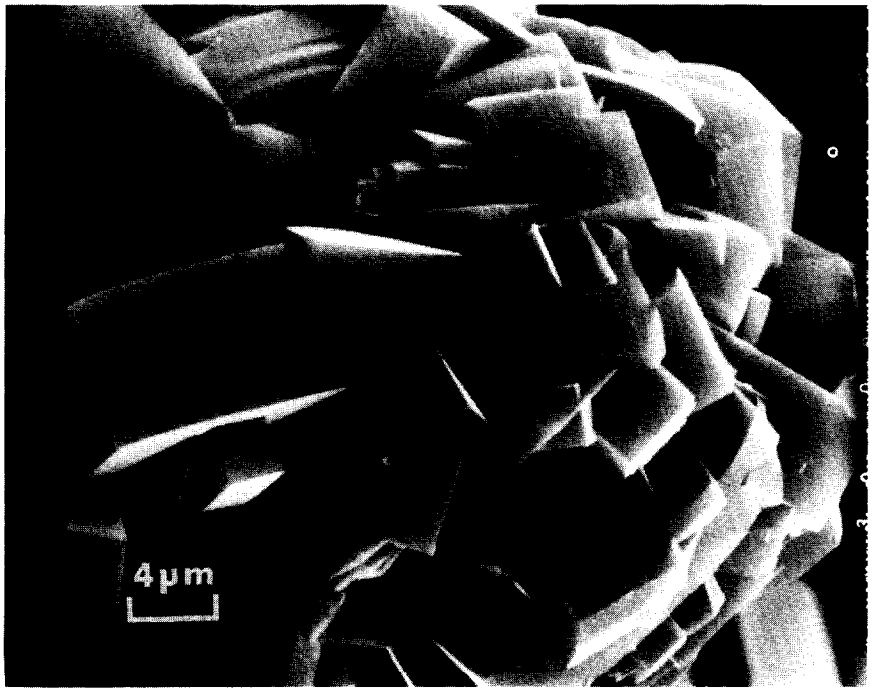

FIG. 20. Scanning electron photomicrograph of the surface of the crystal aggregates grown with the addition of Na_2CO_3 to the reaction mixture.

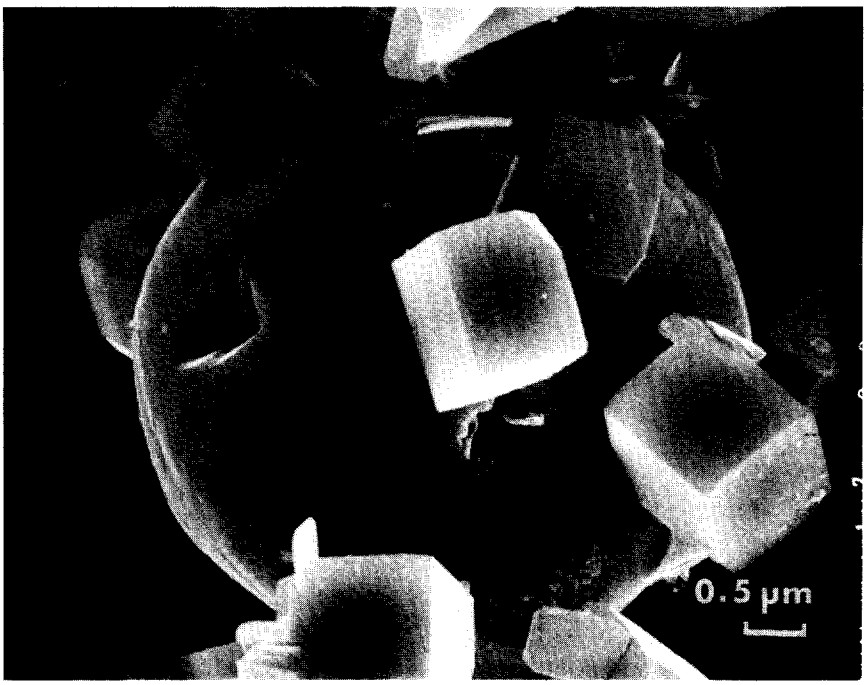

FIG. 21. Scanning electron photomicrograph of the crystals of XSM-5 and "analcime-like" phases grown from a Na_2CO_3 added reaction mixture.

Some exploratory runs were made in the (Na, TPA_2–Al_2O_3–SiO_2–H_2O and (K, TPA)$_2$O–Al_2O_3–SiO_2–H_2O systems, with the starting batch compositions of lower Si/Al and (TPA, Na, K)$_2$O/Al_2O_3 ratios than of those yielding the ZSM-5 phase. A "Na-gismondine-like" phase and an "analcime-like" phase formed after 24 hr in the (Na, TPA) system, and a "K-phillipsite-like" phase formed in the (K, TPA) system. Figures 15 and 16 show the reaction mixture compositions and the phases formed after 24 hr in the (Na, TPA) and (K, TPA) systems, respectively. The X-ray diffraction patterns of the phases are listed in Tables 5, 7, and 8. Figure 17 is the scanning electron photomicrograph of the "K-phillipsite-like" phase.

Pure ZSM-5 crystals were also synthesized from reaction mixtures, in which the TPA ions were replaced with other quaternary ammonium cations, such as TMA, TEA, and TBA. Although sufficient data are not available to give definite conclusions, TMA cations appear to have a stronger "template" or "structure directing" effect than the TEA and TBA ions; a "hydroxy sodalite-like" phase formed whenever TMA was introduced to the reaction mixture. Figure 18 shows the morphology of the pure ZSM-5 phase obtained by replacing 25% of the TPA with TBA ions. The sizes of the aggregate-like ZSM-5 crystals forming from the TPA–TBA batch were about 1.5 μm, larger than those of the ZSM-5 crystals or crystal aggregates obtained using TPA alone. Table 9 lists the X-ray diffraction pattern of the "hydroxy sodalite-like" phase.

Some initial results of a particulation study are worth mentioning. Striking changes in morphology were obtained by the addition of NaCl, Na_2CO_3, and KCl salts to the reaction mixtures in different amounts and under different synthesis conditions. Single crystals and crystal aggregates in the fluidized size range, as well as completely crystallized crystal aggregates in the fixed-bed ranges, changing from 100 to 200 μm in size were observed to form in these systems. Figures 19 and 20 show the crystal aggregates obtained with NaCl and Na_2CO_3 additions, respectively, in rotating autoclaves. Figure 21 illustrates the "analcime-like" phase coexisting with ZSM-5 crystals; Na_2CO_3 was added to the reaction mixture, which was aged for 20 hr and reacted in static autoclaves. A "gismondine-like" phase was added to the metastable phases coexisting with ZSM-5, which formed and dissolved very early in the reaction period, in these synthesis runs with salt additions.

ACKNOWLEDGMENTS

The Chemical Engineering Department of Worcester Polytechnic Institute and the Petroleum Research Fund, for providing financial assistance, and Dr. Harry A. Hoyan of the Research Laboratories of Eastman Kodak, for arranging for the company to donate the tetrapropylammonium hydroxide solutions, are gratefully acknowledged.

Appreciation is expressed to Dr. Ronald R. Biederman for the use of the Jelco Model U3 Scanning Electron Microscope.

REFERENCES

1. Argauer, R. J., and Landolt, G. R., U.S. Patent 3,702,886 (1972).
2. Kokotailo, G. T., Lawton, S. L., Olson, D.H., and W. H. Meier, *Nature (London)* **272**, 437 (1978).
3. Meisel, S. L., McCullough, J. P. Lechtahler, C. H., and Weisz, P. B., *Chem. Tech.*, Feb. 86 (1976).
4. Flanigen, E. M., Bennett, J. M., Grose, R. W., Cohen, J. P., Patton, R. L., Kirchner, R. M., and Smith, J. V., *Nature (London)* **271** (1978).
5. Grose, R. W., and Flanigen, E. M., U.S. Patent 4,061,724 (1977).
6. Erdem, A., M.S. thesis, Department of Chemical Engineering, Worcester Polytechnic Institute (1978).
7. Culfaz, A., and Sand, L. B., *Adv. Chem. Ser.* **121**, 140 (1973).
8. Sand, M. S., Coblez, W. S., and Sand L. B., *Adv. Chem. Ser.* **101**, 127 (1971).